



A Numerical Model of Wet Isotropic Etching of Silicon Molds for Microlenses Fabrication

M. Baranski,^{a,b,z} J. Albero,^a R. Kasztelanic,^b and C. Gorecki^a

^aDépartement MN2S, Institut FEMTO-ST (CNRS UMR 6174/UFC/ENSMM/UTBM) UFR Sciences et Techniques, 25030 Besançon Cedex, France

^bFaculty of Physics, University of Warsaw, 02-093 Warsaw, Poland

A numerical model is proposed to simulate the isotropic wet etching of silicon through an aperture of a mask to produce microlenses molds. The etching process is based on aqueous solutions of HF and HNO₃ in the range of concentrations where etching rate depends mostly on mass-transfer effects. In the considered case the etching rate is defined by diffusion of F⁻ ions to the (oxidized) silicon surface. The simulation is built with the finite element method (FEM) coupled with the level set method (LSM). Our model does not assume an infinite reaction rate on the etched surface. We investigate the influence of finite rate of the reaction on the shape of the etched structures. We investigate 2D and axis-symmetric geometrical cases, properly suited for microlenses fabrication applications. The fitting of the model parameters with experimental data is thus presented. A simplified method to simulate chaotic stirring of the etchant mixture is also proposed to study common experimental setups where the etching baker is agitated. The etching of prefabricated silicon structures is analysed in order to add the possibility of more flexible design of the fabricated structures.

© 2011 The Electrochemical Society. [DOI: 10.1149/2.079111jes] All rights reserved.

Manuscript submitted May 6, 2011; revised manuscript received August 25, 2011. Published October 5, 2011.

Silicon etching is a widely used technique in the fabrication of well-known structures for MOEMS (Micro-Opto-Electro-Mechanical Systems), such as membranes for pressure sensors, cantilevers or via holes.^{1,2} The isotropic wet etching of silicon is characterized by the ideal etching of all its crystallographic planes at the same etch rate. One of the most used isotropic etchants is the solution of nitric acid and hydrofluoric acid. Examples of silicon etched by means of these mixtures are reported in the literature to fabricate channels with curved shapes and bended corners for micro-chromatography³ or to fabricate molds for micro-optical components.^{4,5}

The simulation of the shape evolution of the etched cavities gets to be a complicated issue of silicon wet etching, especially when dealing with transport governed processes coupled with the chemical reaction and the moving boundary. To simulate the etching process, one of the most important aspects is dynamics of material dissolution, in particular if the etching rate is considered constant respect to all physical variables, such as time, structure geometry, crystallographic planes, concentrations of reagents and reaction products. In this case, the simulation would require only one physical parameter, i.e. the etching rate that could be easily measured experimentally. In real systems, the problem is much more complicated. The etching process is governed by chemical reactions that are strongly coupled with physical properties of the materials and with the parameters and inherent characteristics of the etching mixture.

A basic analysis of the etching chemistry in mixtures based on HF/HNO₃ acids divides the process in two stages. Firstly, the silicon surface is oxidized. Secondly, the silicon dioxide is dissolved by reacting with fluoride ion.

In general, the reaction rate is dependent on several factors, such as reagent concentrations, temperature and use of solvents and their concentrations (typical solvents are water and acetic acid). In monocrystalline silicon etching, the etch rate can also depend on the crystallographic orientation of the face exposed to the solution. Several studies show that the crystallographic orientation of silicon affects the etching rate,⁸⁻¹⁰ leading to a certain degree of anisotropy.

Despite the high number of variables that can influence kinetics of the etching process, hardly ever it is necessary to consider all of them. In most cases, it is enough to take into account one or two leading terms to sufficiently describe the dynamics of an experimental setup. It is widely accepted that the dynamics of the etching process are governed by rate-limiting factors, leading to two main groups of processes: reaction limited and transport limited. Reaction-limited cases are those

where the chemical reaction is slower than the transport process (diffusion of reagents to the surface), whereas in transport-limited cases the diffusion is slower than the reaction. Etching characteristics are thus dependent on which one of these factors is dominant. Silicon etching in aqueous solutions of KOH is an example of a reaction-limited system. This type of process is characterized by being almost insensitive to agitation and significantly dependent on temperature. However, in transport-limited systems, etching is highly affected by agitation and in many aspects practically independent on temperature. This is due to the fact that the etch rate is determined by the transport of reacting molecules. Thus, in that regime, the actual speed of the reaction taking place and its dependence on the mentioned parameters is often negligible. In the presented work we consider the etching process where both terms are present. The considered system is transport-dominated but not a priori transport-limited. Finite reaction rate considered in the model influence the etching characteristics.

The aim of this paper is to propose a numerical analysis of silicon wet isotropic etching with HF/HNO₃ mixtures through an aperture of a mask, demonstrating its pertinence with a concrete application. When etching with this kind of solutions, the proportion of each acid used in the mixture plays a crucial role in etching characteristics.^{6,8,11-14} A special interest lies in low HF concentration regime of the solution, often called “polishing regime”, because it produces high quality surfaces. The application investigated in this paper profits from these characteristics, aiming to produce microlenses by means of micro-molding techniques.^{4,8,15}

The paper is structured as follows: firstly simplified model of the etching process is presented secondly mathematical description of the problem is formulated and employed numerical methods are described. Followed by section presenting the experimental verification of the model. Finally, more complicated geometrical cases are discussed, the conclusions and perspectives of this work are given.

Simplified Model of the Process

The scope of this paper is the numerical study of silicon isotropic etching in a solution composed by HF and HNO₃, applied to the fabrication of microlenses molds. In micro-optics applications high quality surface of the molds are required, i.e., with a very low roughness. We therefore consider the appropriate etch solution characterized by low HF concentration ($C_{HF} \approx 3 \text{ mmole/cm}^3$) and high HNO₃ concentration ($C_{HNO_3} \approx 25 \text{ mmol/cm}^3$). The expected range of average surface roughness (R_a) when a Si wafer is etched in these conditions is in the order of several nanometers.^{6,8,15}

^z Email: maciej.baranski@femto-st.fr

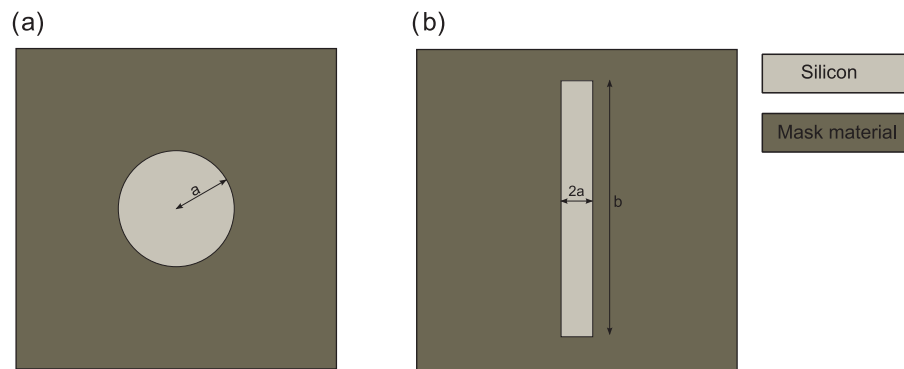


Figure 1. Two considered geometrical cases defined by the shape of the mask opening (a) circular - radial symmetry and (b) rectangular which is approximated by 2D model with transversal symmetry along length of the structure.

The etching process can be simplified in case of a mixture with low concentration of HF and high concentration of HNO_3 . In this case, the oxide dissolution step is a rate-limiting factor of the process. The silicon oxidation reaction rate does not influence the kinetics of the etching process, due to a high reaction constant, low stoichiometric ratio of oxidation reaction and higher concentration of HNO_3 used in the mixture.⁸ In the considered system etching through a mask, the etching is analyzed as if it would be a single step reaction process. It is important to underline that this approximation is only valid for the situations with high HNO_3 concentration. The region in which the model is valid can be found with a maskless etching experiment, where the dependence of etching rate with concentrations can be investigated.¹² In systems where HNO_3 concentration is not high enough etching may be influenced by the oxidation reaction. And oxidation reaction is likely to have anisotropic character because it acts directly on the crystal structure of silicon in contrast to dissolution of the amorphous silicon oxide.

The model is applicable in the range of compositions where the etch rate is constant, regarding HNO_3 and solvent concentrations. The etching mixture that we are considering is composed by aqueous solutions of HF (49%wt.) and HNO_3 (68%wt.) in proportion 1:9. According to data from Schwartz and Robbins, it fulfills the condition of validity for the one-step reaction process approximation.¹² In these conditions, the etch rate depends on the transfer of fluoride ions onto the oxidized silicon surface. Consequently, the mass transport in the solution governs etching kinetics.

Mathematical Formulation

A qualitative analysis of the chemistry concerning the described etching process makes possible the consideration of process kinetics as a transport problem that can be mathematically formulated. The diffusion as a main transport phenomenon can be considered by the mathematical formulation:

$$\partial_t C = D \Delta C \quad [1]$$

where C is the concentration distribution in mole/cm^3 , D is the diffusion coefficient in $\mu\text{m}^2/\text{min}$, and t is the time. Equation 1 describes the evolution of the concentration distribution with time that takes place due to the random movement of molecules in the solution. To describe the transport mechanism in terms of differential equations, it is necessary to take into account the boundary and initial conditions that are defined by the domain of the problem. Four boundary conditions appear in our case: constant concentration in bulk solution, zero flux of reagents through an impermeable mask, concentration and the etching rate on the reacting surface.

Two main geometrical cases considered in the work: circular mask used for fabrication of axially symmetrical lenses and long rectangular mask employed for fabrication of the cylindrical lenses (Fig. 1). For circular mask opening axially symmetrical model is used. For rectangular mask opening translational symmetry can be used only if the length of the structure is large enough in comparison to the diffusion length in the system ($b \gg 2\sqrt{Dt}$). Influence of the finite

length of the rectangle is visible only close to shorter borders of the rectangle.

Besides diffusion, other mass transfer sources can become important in the wet etching problem. For instance, those related to the flow of the solution, i.e. large-scale movement of the etchant that can be caused by density gradients of liquid, arising from the etching process itself (generation of heat and dense reaction products). A way often used in microfabrication to enhance the transport of reagents to the etching area is the mechanical agitation of the etching solution. This is a simple method that allows some control over the etch rate, since diffusion and natural convection movement are practically uncontrollable. In microlenses fabrication technologies, the symmetry of the final structure is very important and a disadvantage of mechanical stirring by commercially available agitators is that symmetry can be easily lost. Asymmetry can be minimized only if the mixing is random and do not favor any direction. This can be obtained by chaotic mixing when etching baker is randomly shaken.

According to the previous consideration, we discuss two different cases of mass-transfer. In the first one, the mass-transfer is only due to the diffusion, i.e., the diffusion layer is much thicker than the size of the etching area. The aim of the later is to introduce the finite size of the diffusion layer in the context of the considered experimental setup, in which the agitation is performed manually.

A strict mathematical formulation of the physical problem of that kind of agitation would require the inclusion of fluid flow terms into the equation of the concentration distribution evolution. Therefore, it would lead to an advection-diffusion equation coupled with the Navier-Stokes equation, which describes the flow of the etchant.¹⁶ However, the formulation of the precise boundary conditions of the fluid flow calculation for the described manual mixing is practically impossible.

In the method used here we consider only the average effect of the fluid flow on the concentration field that governs the etching process. Because the etching mixture is considered as a viscous liquid and the structures to be generated are sufficiently small (from 5 to 500 microns), it is assumed that fluid flow of the etching mixture does not affect the concentration field in the direct neighborhood of the structure. As a consequence the diffusion layer develops in finite distance above the etched area.

A particular case where the thickness of the diffusion layer is introduced due to the agitation is time variant. Time dependence of the boundary layer intends to reflect the periodic character of the agitation (shaking the etching baker) and adds the second parameter characterizing the agitation - first parameter commonly used exclusively to describe the agitation is the thickness of the boundary layer. In the presented work the time dependence of the agitation is constructed as the periodic perturbation of the diffusive mass transfer problem. The concentration field developed by the diffusion is periodically 'reset' (with period τ) above the boundary layer (of thickness d).

This simplification is justified by the experimental repeatability of the structures noticed when the solution is stirred manually. In that case, mixing is different in every process in terms of fluid flow. However, the repeatability of the fabricated structures between processes

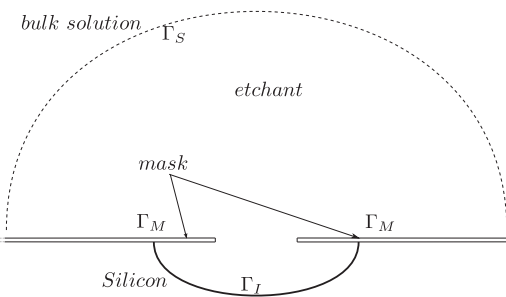


Figure 2. Geometry of the considered problem. Γ_M is the boundary defined by the mask position, Γ_I is the etching interface and Γ_S is the boundary representing bulk solution, which is the source of the fresh etchant.

has been demonstrated.¹⁵ To simulate a stirred process, we use an average influence of mixing on the reagents concentration distribution, without direct consideration of the fluid flow of the etchant.

Solution method and the boundary conditions.— To model transport-governed etching systems, several methods have been discussed in the literature. An analytical solution was introduced by Kuiken^{17,18} with the assumption of an infinitely fast reaction rate ($k \rightarrow \infty$), limited to simple geometrical cases and for long or very short etching time under the assumption of the stationary (not stirred) solution.

The main issue in the etching problem is the moving boundary, which requires special considerations when conceiving the numerical solution. We use a numerical grid in order to define the computational domain for the numerical solution of the transport problem. The moving grid method¹⁹ used in this work decouples concentration evolution and geometry expansion to be solved separately, one independent of the other within one time step. The concentration distribution on the fixed grid is solved with the finite element method (FEM) whilst geometry evolution is calculated with the level set method (LSM).^{20,21} The LSM is also the core of the dynamic meshing technique used in the simulation.²² The symmetry of the considered geometries (translational of the slit and radial in circular) can be described as 2D cases (whose geometry is shown in Fig. 2) in order to reduce the computational load and simplify the meshing algorithm.

The boundary condition on the reacting surface is defined by equilibrium of the diffusive flux and reacting flux of the reacting species:¹⁹

$$D \frac{\partial C}{\partial \vec{n}} = kC \quad [2]$$

where k is the surface reaction rate constant expresed in $\mu\text{m/s}$. Equation 2 describes then the concentration behavior on the etching boundary. The reaction rate could be a complex function of many variables. In our model, we assume that k is a constant, scalar value. Equation 2 is often simplified to $C=0$ on the etching surface. This is a consequence of assuming an infinitely fast reaction rate. However, a strict mathematical formulation requires a condition that compares the reaction rate with diffusion speed. For this purpose, a characteristic length scale (L) has to be introduced. In consequence, this approximation suffers scale dependence and it can be applied only when the following condition is satisfied:

$$\frac{D}{k} \ll L \quad [3]$$

where L is the length scale of the considered process. The traces of anisotropy observed by Schwartz and Robins⁸ and investigated by Svetovoy et al.¹⁰ can be caused by the violation of the condition 3, whereas they cannot be explained with a single scalar reaction rate approximation.

Another boundary condition on the etching surface is the so-called Stefan condition.¹⁹ It is introduced to describe the boundary evolution caused by the etching process. The best way to describe the evolution of the surface (curve in 2D) is to define the normal velocity distribution v_n that is directly related to the flux of reacting species, since etching rate is linear regarding the number of reacting molecules:

$$v_n = \gamma \phi_R \text{ with } \gamma = \frac{M_{Si}}{n \rho_{Si}} \quad [4]$$

where γ is the factor that transforms molar units into volumetric units, and it is defined by the silicon molar mass M_{Si} , the silicon density ρ_{Si} and the stoichiometric ratio $n = 6$, because a single silicon particle is dissolved by 6 F^- ions to form one SiF_6^{2-} ion released to the solution.

Equation 1 together with boundary conditions defined on etching area 24, on the mask border $\frac{\partial C}{\partial \vec{n}} = 0$ and the bulk solution $C = C_0$ forms complete mathematical description of the diffusion governed etching system.

Dynamic geometry description.— The mathematical formulation defined in section 3.1 requires a solution for transport equations on expanding geometry. One of the tools to describe evolving shapes is the level set method (LSM) introduced by Sethian and Osher.^{20,21} The main idea behind LSM is to change the curve evolution into the evolution of a 2D function:

$$V_n |\nabla \Phi| = -\partial_r \Phi \quad [5]$$

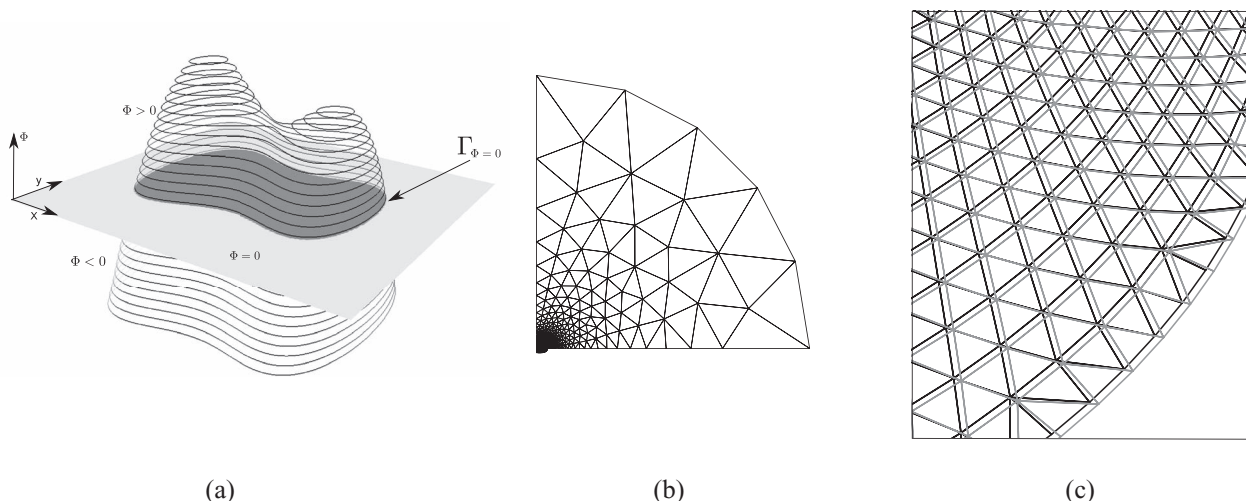


Figure 3. Level set function used for geometry definition (a), grid used for the FEM calculations - whole computational domain (b) and the detail of the mesh for two different time steps (c).

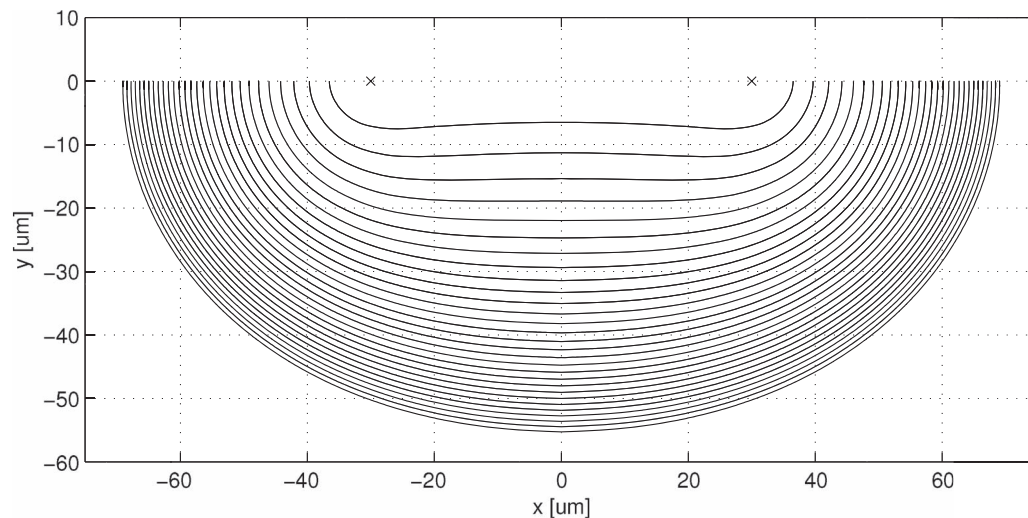


Figure 4. Simulation of etching through a circular mask ($a = 30 \mu\text{m}$). Shape profiles are plotted with time steps $\Delta t = 1 \text{ min}$. The etching rate is non-uniform across the structure and in addition it slows down in time. The positions of maximal values move from regions near the mask at the beginning of the process towards the center of the structure at the end.

where Φ has no physical interpretation except at the zero level, where it describes the curve:

$$\Gamma_I = \{\vec{x} \mid \Phi(\vec{x}) = 0\} \quad [6]$$

V_n in equation 5 is the normal speed distribution extended from a curve to a whole plane:

$$v_n = V_n(\Gamma_I) \quad [7]$$

where v_n is defined only at the silicon surface.

The LSM formalism can be also used to define the geometry. The level set function has different signs inside and outside the space defined by the curve. The construction of the function $\Phi(\vec{x})$ is done as a signed distance function (SDF) that maps distances to the closest point on the curve. Its gradient has a magnitude equal to 1 and it points towards the direction of the nearest point on the curve (fig. 3a).

The natural way in which LSM defines curves and areas, as well as the simplicity to find the direction and distance to the boundary,

makes possible to use it as the base for the grid generator. Moreover the combination of LSM and FEM makes possible the handling of dynamic geometries.²²

Simulation Scheme

The numerical solution that we propose is based on decoupling the mass transfer problem and the geometry evolution, as it has been introduced in the previous section. For each single time step of the simulation, the concentration distribution is first calculated on the stationary grid and afterwards the geometry is updated due to the etching. The mathematical justification for decoupling those equations relies on the fact that etching is much slower than diffusion.¹⁷ Typical values of the etching rate in the investigated mixtures are up to several microns per minute. Diffusion length at the concerned spatial and temporal scales is about 100 microns.

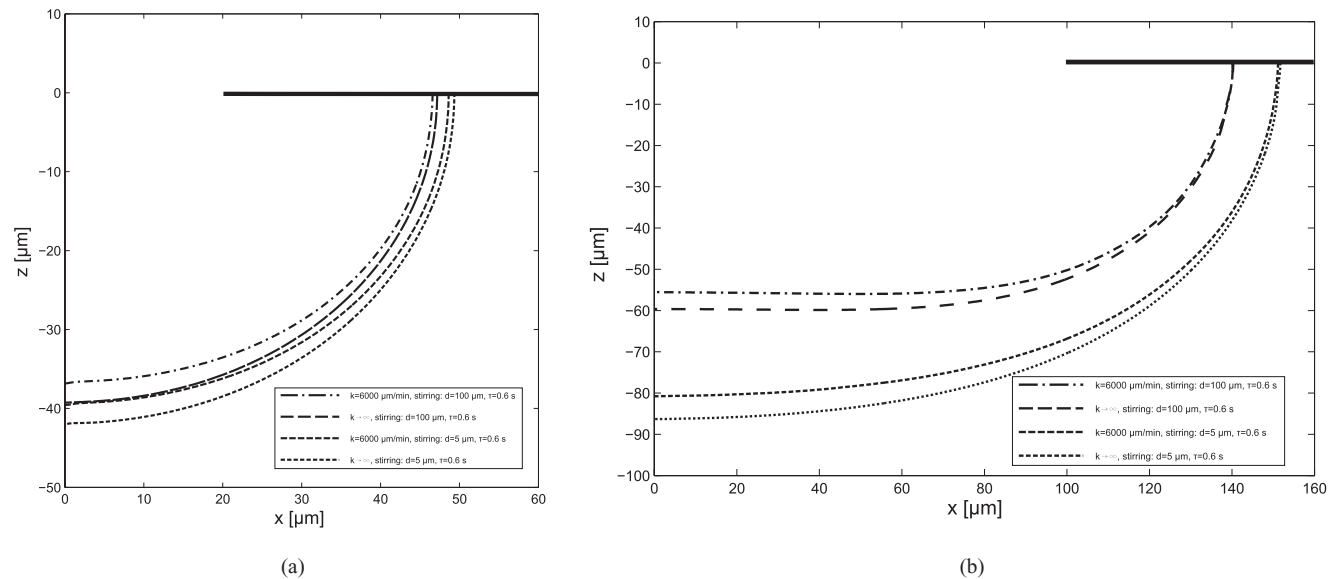


Figure 5. Influence of finite reaction rate and stirring the etching mixture on the etched cavities in case of etching through a circular mask with $r = 20 \mu\text{m}$ for $t = 10 \text{ min}$ (a) and $r = 100 \mu\text{m}$ for $t = 20 \text{ min}$ (b)

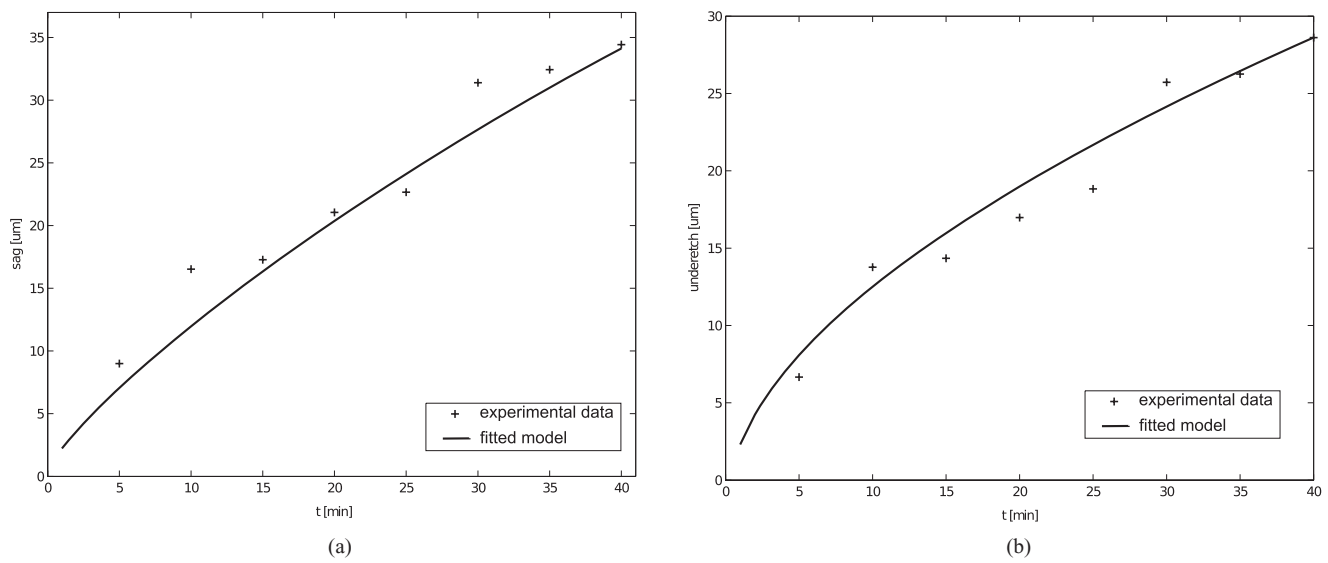


Figure 6. Time evolution of the structures, (a) depth (*Sag* of the final microlens) and (b) increment of the aperture radius at the surface level (*underetch*).

Expanding the computational domain within the FEM framework requires control of the quality of the triangular mesh that describes the geometry of the structure. The implicit function used for tracking the etch-front propagation allows a simple optimization of the nodes position during the expansion of the geometry, keeping that way a high quality of the mesh (defined as a small gradient of triangle sizes and the limit of minimal triangle angle in the whole mesh) at every moment of the simulation. Figure 3b illustrates two meshes used in different time steps of the simulation. An additional issue of changing the mesh during simulation is the need of transforming the concentration distribution from one grid into a new one at the following time step. For this purpose, two methods can be used. The first one consists on adding numerical advection to the transport equation and afterwards solving the advection-diffusion equation with the velocity defined by the motion of the mesh. An alternative method is to interpolate variables from the old mesh to the new one. The second method is slower than the first one since it introduces additional computation to the simulation, but it does not require nodes tracking. Thus, it needs less effort to resolve the mesh adaptation during the

simulation. Therefore, we preferred the interpolation method to be implemented.

LSM is used to describe the geometry evolution, and therefore the numerical domain of the Level Set function can be limited to the small area where it actually evolves, i.e. close to the mask aperture. Furthermore, the Level Set function is used for the meshing algorithm, thus it has to be defined on the whole domain of the FEM calculation of concentration evolution. The implemented method divides the LSM domain into two different parts. The first part describes the stationary geometry of the bulk solution and can be defined by an analytical function. The second part describes the evolving part of the domain and it is defined and solved numerically on a Cartesian grid.²³ This method allows using the LSM to describe the whole geometry, but at the same time it limits the grid size used for the computations.

Three main step compose the simulation. In the first step, the concentration distribution is calculated by solving the mass transport equations using FEM. The second step consists on calculating the etch rate distribution on the silicon surface with equation 4. In the last step, the geometry evolution is calculated with the LSM and the mesh

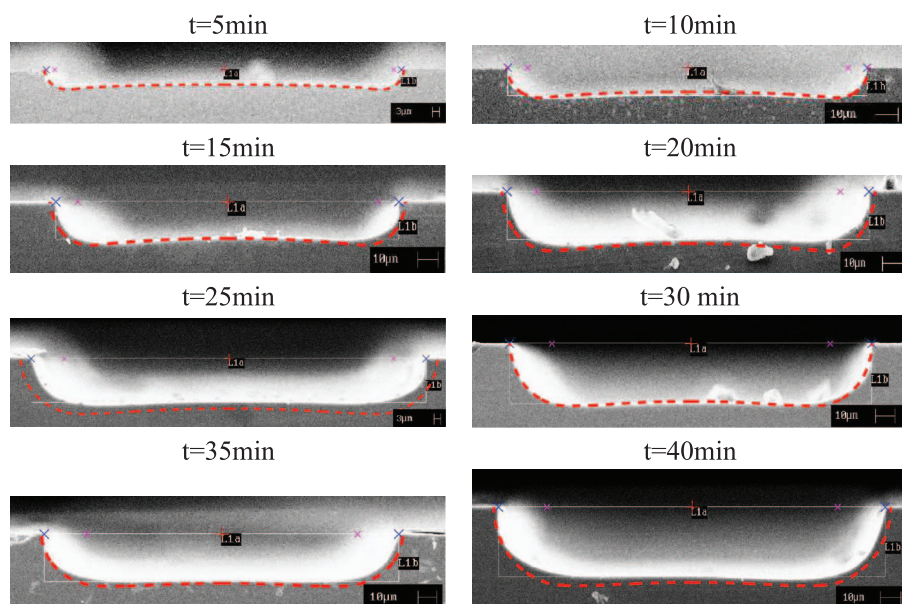


Figure 7. SEM pictures of the cross-section of etched structures through a mask aperture with the shape of a rectangle. The shape calculated from the model is shown as the superimposed dashed line.

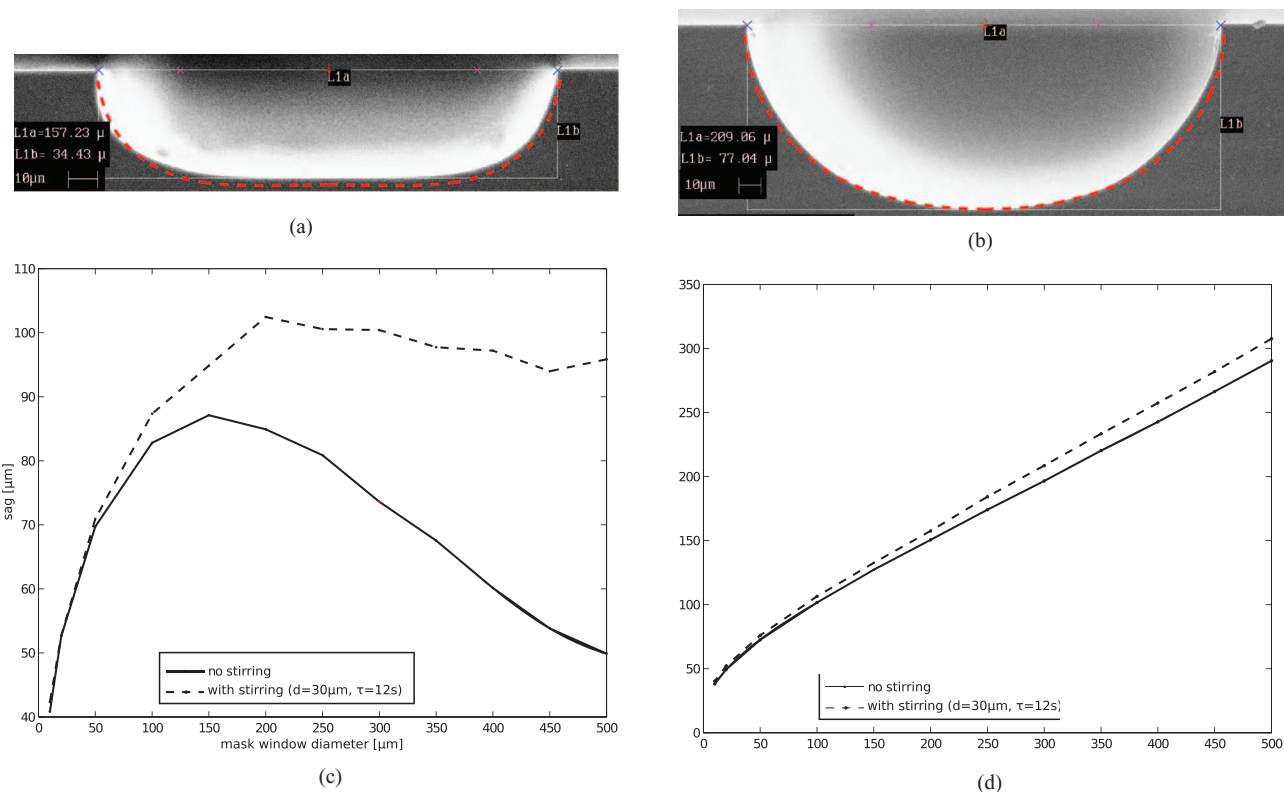


Figure 8. Effect of stirring the etching mixture. The process speeds up and changes characteristics of etch rate distribution, both effects with respect to a particular mold (a) and (b), and also with respect to the structure size (c) and (d). The agitation parameters $d = 30 \mu\text{m}$ and $\tau = 12 \text{ s}$ used for the simulation describe properly the investigated process of molds fabrication.

is corrected to fit the new computational domain. The simulation result is the evolution of the structure shape etched under the given conditions: etching time, HF concentration, aperture shape and size and the mixing parameters (Fig. 4).

Described algorithm was implemented in MATLAB employing Level Set toolbox by Mitchell²³ and mesh generator based on mesh generator for implicit defined domains by Persson.²²

Numerical Results and Experimental Verification

To verify the model, the experiments were performed with (111) plane oriented silicon pieces containing the two geometries of mask apertures: circular and rectangular (Fig. 1). The sizes were ranging from 5 to 500 microns (diameter of the circles and width of the rectangles). Experimental data were used in order to find the physical parameters of the model (k , D) as well as to test the range in which the assumptions for derivation are valid. The parameters of the fitting

model are based on time dependence of the structure depth and radius, revealing values in order of $D \approx 6 \times 10^4 \frac{\mu\text{m}^2}{\text{min}}$ and $k \approx 6 \times 10^3 \frac{\mu\text{m}}{\text{min}}$. The diffusion coefficient is close to the value of water-dominated systems. The fitted value of the surface reaction rate k according to equation 3 lies in the range where it has not a negligible impact in etching characteristics.

In case of pure diffusion governed process only the structures much larger than $10 \mu\text{m}$ the assumption of the infinite reaction rate may be used. In the case of stirred process boundary layer thickness is more appropriate length scale to characterize the transport process. The effect of the finite value of the reaction rate depends on the size of the structure and the intensity of the stirring. In case of relatively big apertures (Fig. 5b) reaction rate influence the etching mainly in the center of the structure. For smaller structures (Fig. 5a) whole shape is affected. The theory with assumption of $k = 0$ investigated by Svetovoy et al.⁹ gives very good prediction of the underetch length however as figure 5 shows the most important changes due to finite

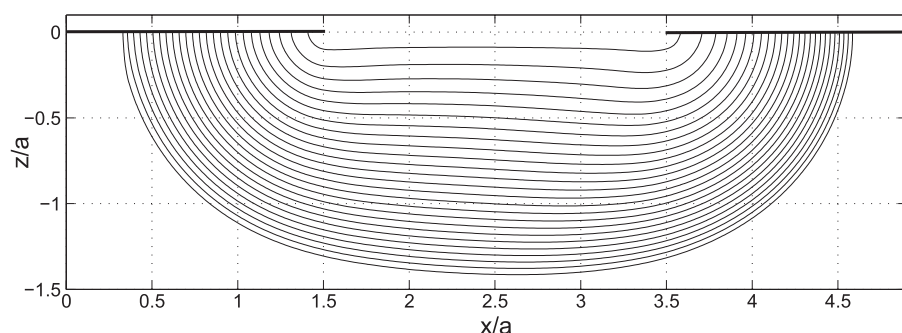


Figure 9. Slight asymmetry of the etched structure caused by neighborhood effect. Shapes of the structure (linear mask $a = 50 \mu\text{m}$) etched in direct neighborhood of another similar structure. The second structure (not shown in the figure) is symmetrically reflected relative to $x = 0$ axis.

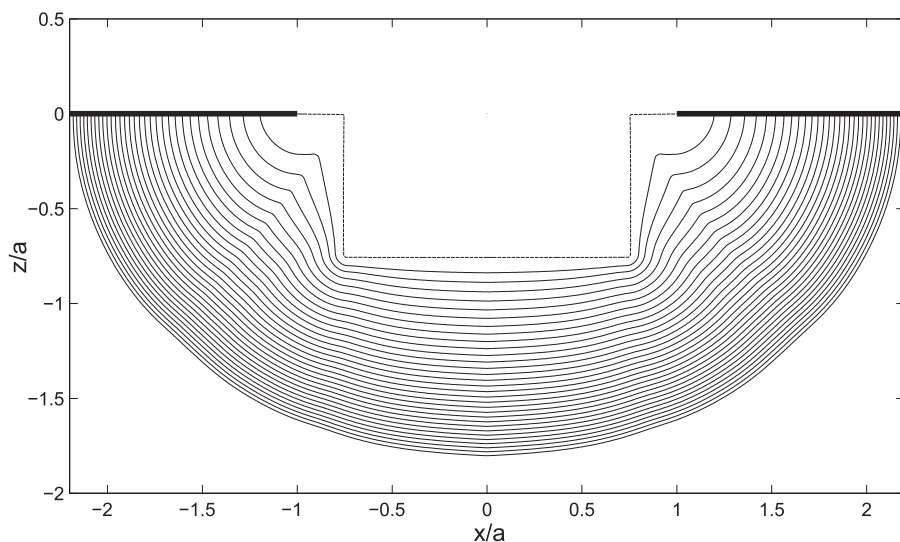


Figure 10. Etching profiles of the structure with cylindrical hole ($r_{hole} = 37.5 \mu\text{m}$, and height $h_{hole} = 37.5 \mu\text{m}$) in the center of the mask aperture with radius $a = 50 \mu\text{m}$. Dashed lines indicate initial shape of the structures, thick lines indicate the position of the mask.

value of k are pronounced in the center of the structure. The influence of the stirring on the etching process is caused by acceleration of the transport of reagents to the etched surface and as that it also amplify the effects of finite reaction rate that takes place on the etching surface. The geometrical dependence of the finite value of k is especially important when consider large structures or more complicated shapes like etching prefabricated structures (Fig. 10). The under-etching in all cases is less sensitive to the value of k than the depth of the mold. This is explained by the fact that when etching deep structure mass transfer is less effective to the corner of the mold than to area located directly below the mask opening.

The comparison between the model and fabricated structures is shown in figures 6a and 6b. The time evolution of characteristic lengths in the structure during the process shows a good agreement with the time dependence of the etch rate. The cross-section of the experimental structures for different etching times with the superposition of the calculated profiles is presented on Fig. 7. The images show that the whole structure shape is well predicted by the model. The differences appearing between simulated and experimental shapes are mainly due to the motion of the etching mixture. Those differences can be explained by the fact that the fluid flow can cause asymmetry in the generated cavities.²⁴ In this regime, the introduction of neglected factors such as a complex dependence of k respect to the etching variables (such as reaction products concentration or the crystallography of the etched material) does not improve the result significantly. The symmetry can be significantly restored when chaotic (non directional) stirring is applied (Figs 8a and 8b). Another effect due to the advection is the change of scale dependence in the etching characteristics. Mixing affects weakly the small structures and speeds up the etching rate significantly in larger structures (Figs 8c and 8d). In addition, the etching rate increases at the center of the structure, resulting in a change of the structure aspect ratio towards hemisphericity, which is therefore giving a very important improvement in terms of the optical performance of the fabricated microlenses.

Advanced Geometrical Cases

In the following section more complicated geometrical cases are discussed. In the subject of MOEMS device design and fabrication arrayed version of lenses are often considered. In case molding technique used for lenses fabrication it means fabricating many molds close to each other. In the considered etching process proximity of two etched structures influences the results of the etching. Neighborhood effect⁶ can cause asymmetry in the fabricated structures (Fig. 9). This phenomenon usually considered as highly unwanted effect. Often additional compensation structures are added to eliminate

the asymmetry however in this case the etching characteristics are different than in the case of the single structure.

Main limitation of the mold fabrication with etching through simple circular mask opening is limited possibility of design of mold shape. An idea that allows flexible design of the shape of the final structure is the etching process of prefabricated 3D structure. In figure 10 evolution of profiles obtained by etching a cylindrical hole placed in the center of the circular mask is presented. This approach significantly improve the sphericity of the final mold especially for large mask openings where in standard conditions very long etching time is necessary to obtain the mold with uniform curvature. Using more complicated initial conditions for the wet etching process allows fabrication of molds with more advanced geometry which is promising approach for fabrication the aspheric lenses.

Conclusions

Simplified model of the silicon etching by aqueous solution of HNO_3 and HF was investigated. It is based on observation that etching rate do not depend on concentration of HNO_3 in the regime of low ratio of HF to HNO_3 concentrations in the etching mixture. As consequence etching is modeled as single step process determined by transport of HF to the etched surface. Reaction rate influence into the etching characteristics is discussed. It is shown that it have non negligible effect into the final shape of the fabricated mold. The etching systems with mechanical stirring have been modeled with an simplified method based on the average effect of the fluid flow. This method reproduces the most important effects observed in the etching in a stirred mixture i.e. etch rate acceleration, aspect ratio changes and structure scale characteristics. Two examples of more advanced geometrical cases were discussed. The first one investigate the neighborhood effect that appear when one structure is etched in direct proximity of another. The second one discuss the etching process of the complicated silicon structures. This approach allows advanced shape design of the fabricated mold. Future perspective of the presented work will be focused on fabrication of molds for aspheric microlenses.

Acknowledgment

We would like to thank Madoka Hasegawa for reading and discussing the manuscript.

References

1. Greenwood, J., *J. Phys. E: Sci. Instrum.*, **17**, 680 (1985).
2. Dantas, M. O. S., Galeazzo, E., Peres, H. E. M., Ramirez-Fernandez, F. J. *Eletrochem. Soc. Proc.*, **2003-09**, 445 (2003).

3. J. Dziuban, A. Gorecka-Drzazga, L. Nieradko, K. Malecki, *J. Capillary Electrophor. Technol.*, **6**, 37 (1999).
4. Albero, J., Nieradko, L., Gorecki, C., Ottevaere, H., Gomez, V., and Pietarinen, J., *Proc. of the SPIE*, **6992**, 69920A-69920A-9 (2008).
5. Albero, J., Gorecki, C., Nieradko, L., Päävänrananta, B., Gomez, V., Thienpont, H., and Passilly, N., *J. of the European Optical Society – Rapid Publications*, **5**(10001) (2010).
6. Tjerkstra, R. W., PhD Dissertation, Micromechanical Devices of the MESA Research Institute at the University of Twente, Enschede, The Netherlands (1999).
7. Steinert, M., Acker, J., Oswald, S., and Wetzig, K., *J. Phys. Chem. C*, **111**(5), 2133 (2007).
8. Schwartz, B. and Robbins, H., *J. Electroch. Soc.*, **108**(4), 365 (1961).
9. Svetovoy, V. B., Berenschot, J. W., and Elwenspoek, M. C., *J. Electroch. Soc.*, **153**, C641 (2006).
10. Svetovoy, V. B., Berenschot, J. W., and Elwenspoek, M. C., *J. Micromech. Microeng.*, **17**, 2344 (2007).
11. Gad-el-Hak, M., [The MEMS Handbook: MEMS, design and fabrication], ch. 3.7: MEMS Fabrication, Wet Isotropic and Anisotropic Etching, Richmond, CRC Press (2006).
12. Schwartz, B. and Robbins, H., *J. Electroch. Soc.*, **106**(6), 505 (1959).
13. Schwartz, B. and Robbins, H., *J. Electroch. Soc.*, **107**(2), 108 (1960).
14. Schwartz, B. and Robbins, H., *J. Electroch. Soc.*, **123**(12), 1903 (1976).
15. Albero, J., Nieradko, L., Gorecki, C., Ottevaere, H., Gomez, V., Thienpont, H., J.Pietarinen, B.Päävänrananta, and Passilly, N., *Optics Express*, **17**(8), 6283 (2009).
16. Patankar, S. V., [Numerical heat transfer and fluid flow], Hemisphere Pub. Corp. New York (1980).
17. Kuiken, H. K., Kelly, J. J., and Notten, P. H. L., *J. Electroch. Soc.*, **133**(6), 1217 (1986).
18. Kuiken, H. K., *J. Eng. Math.*, **45**(1), 75 (2003).
19. Vermolen, F. J., Vuik, C., Javierre, E., and van der Zwaag, S., *Nonlinear Analysis: Modelling and Control*, **10**, 257 (2005).
20. Sethian, J., [Level Set Methods and Fast Marching Methods Evolving Interfaces in Computational Geometry, Fluid Mechanics, Computer Vision, and Materials Science], Cambridge University Press (1999).
21. Osher, S. and Fedkiw, R. [Level Set Methods and Dynamic Implicit Surfaces], Berlin, Springer (2003).
22. Persson, P.-O. and Strang, G., *SIAM Review*, **46**(2), 329 (2004).
23. Mitchell, I. M., *J. Scientific Computing*, **35**(2), 300 (2008).
24. Shin, C. B. and Economou, D. J., *J. Electroch. Soc.*, **138**(2), 527 (1991).